SAR and QSAR in Environmental Research
Publication details, including instructions for authors and subscription information:
http://www.informaworld.com/smpp/title~content=t716100694

Molecular simulation of polycyclic aromatic hydrocarbon sorption to black carbon

J. J. H. Haftka [a]; J. R. Parsons [a]; H. A. J. Govers [a]
[a] Earth Surface Sciences, Institute for Biodiversity and Ecosystem Dynamics, Universiteit van Amsterdam, 1018 WV Amsterdam, the Netherlands

Online Publication Date: 01 April 2009

To cite this Article Haftka, J. J. H., Parsons, J. R. and Govers, H. A. J.(2009)'Molecular simulation of polycyclic aromatic hydrocarbon sorption to black carbon',SAR and QSAR in Environmental Research,20:3,221 — 240
To link to this Article: DOI: 10.1080/10629360902949336
URL: http://dx.doi.org/10.1080/10629360902949336

SAR and QSAR in Environmental Research
Vol. 20, Nos. 3–4, April–June 2009, 221–240

Taylor & Francis
Taylor & Francis Group

Molecular simulation of polycyclic aromatic hydrocarbon sorption to black carbon

J.J.H. Haftka*, J.R. Parsons and H.A.J. Govers

Earth Surface Sciences, Institute for Biodiversity and Ecosystem Dynamics, Universiteit van Amsterdam, Nieuwe Achtergracht 166, 1018 WV Amsterdam, the Netherlands

(*Received 5 February 2009; in final form 30 March 2009*)

Strong sorption of hydrophobic organic contaminants to soot or black carbon (BC) is an important environmental process limiting the bioremediation potential of contaminated soils and sediments. Reliable methods to predict BC sorption coefficients for organic contaminants are therefore required. A computer simulation based on molecular mechanics using force field methods has been applied in this study to calculate BC sorption coefficients of polycyclic aromatic hydrocarbons (PAHs). The free energy difference between PAHs dissolved in water and in water containing a model structure of BC was calculated by thermodynamic integration of Monte Carlo simulated energies of transfer. The free energies were calculated with a hypothetical reference state that has equal free energies in both phases and is therefore cancelled in the calculated free energy difference. The calculated sorption coefficient of phenanthrene (log $K_{BC} = 5.17 \pm 0.54$ L/kg C), fluoranthene (6.33 ± 0.64 L/kg C) and benzo[*a*]pyrene (7.38 ± 0.36 L/kg C) corresponded very well to experimental values available in the literature. Furthermore, an average spacing distance of 3.73 Å between PAHs and BC was determined that is only slightly lower than an experimentally determined value of 4.1 Å. The method applied in this study enables the calculation of the extent of PAH sorption to a soot surface for which no experimental values are available nor data for related compounds as required in quantitative structure–activity relationships.

Keywords: PAH; molecular simulation; Monte Carlo; free energy; statistical mechanics

1. Introduction

The application of force field methods in molecular simulation can provide detailed insights into interactions between hydrophobic organic contaminants and environmental sorbents. The use of force fields to calculate molecular interactions allows the direct calculation of molecular properties without using quantitative structure–activity relationships (QSARs) or artificial neural networks. Previously, force fields based on molecular mechanics have been applied in our group to calculate enthalpies of transfer of organic contaminants to dissolved organic carbon [1,2] and to membrane lipids [3]. Also, force field methods were applied to predict product profiles for the hydroxylation of monoterpenes by the enzyme cytochrome P450cam [4]. The force field method is applied

*Corresponding author. Email: J.J.H.Haftka@uva.nl

ISSN 1062–936X print/ISSN 1029–046X online

DOI: 10.1080/10629360902949336
http://www.informaworld.com

in this study to the calculation of the extent of sorption of polycyclic aromatic hydrocarbons (PAHs) to a model structure of black carbon (BC). These compounds are chosen because they are considered representative members of planar hydrophobic organic contaminants.

In the concept of dual-mode sorption of hydrophobic organic contaminants in the natural environment, organic matter is composed of one domain representing linear and non-competitive *ab*sorption in amorphous organic matter at high sorbate concentrations and a second domain showing nonlinear and competitive *ad*sorption to BC at low sorbate concentrations. Soot and charcoal are commonly termed BC and originate from incomplete combustion of fossil fuels or biomass. These sorbents are part of a group called carbonaceous geosorbents (also including unburned coal, kerogen and coke) and are ubiquitously present in soils and sediments [5–7]. It has been recognised in the past decades that the bioavailability of (planar) hydrophobic organic contaminants is decreased due to strong sorption to these sorbents. This process results in nonlinear sorption isotherms at relatively high contaminant concentrations, multiphasic desorption kinetics, elevated total organic carbon–water distribution coefficients and limited bioremediation potential [6].

Several molecular simulation studies have used model structures of natural organic macromolecules such as humic and fulvic acids [8–14] or representations of soot [8,15,16] to calculate interactions with environmental contaminants. Most of these studies interpreted these interactions with respect to the formation of the most stable structure with the lowest energy. Moreover, the type of bonding between sorbate and sorbent, orientations of the sorbate and conformations of the sorbent involved in the interactions were evaluated in these studies [8,9,11,12,14,15]. Only a few studies directly calculated equilibrium sorption coefficients for the partitioning of polar and nonpolar organic contaminants between humic acids and water, $K_{HA,water}$ (see [10]), or between humic acids and air, $K_{HA,air}$ (see [13]).

In molecular simulations performed by Kubicki [16], quantum mechanical calculations were used to simulate the sorption of benzene (Bz) and PAHs to a model structure of soot (coronene; $C_{24}H_{12}$). In these simulations, differences in partitioning energies were successfully correlated with experimental sorption data obtained from literature for the adsorption of PAHs to diesel soot, $K_{BC,water}$ [5,17]. The calculated energy changes were approximated to changes in enthalpy (ΔH) and changes in entropy (ΔS) were neglected [16]. Both of these thermodynamic properties have to be estimated, however, to calculate a change in Gibbs free energy (ΔG). The sorption coefficient can subsequently be calculated via $\Delta G = -RT \ln K_{BC,water}$. Gibbs free energy can however not be calculated directly from a molecular simulation because a statistically significant sampling of conformation space has to be performed [16]. For a liquid phase containing a sorbate and a sorbent, Gibbs free energy can be assumed equal to the Helmholtz free energy (ΔF) which is related to the canonical partition function as defined in statistical mechanics [18].

Force field calculations using statistical mechanics can therefore be used to predict the sorption behaviour of PAHs to BC, which is determined by differences in Helmholtz free energy between PAHs dissolved in water and in water containing BC. In this study, a method is presented for the calculation of BC sorption coefficients for phenanthrene (Phe), fluoranthene (Fla), and benzo[*a*]pyrene (BaP) using statistical mechanics and can in principle be applied to other PAHs or (a)polar compounds as well. Thermodynamic integration of Monte Carlo ensemble averages over a coupling parameter is applied to calculate free energy differences for the sorption of PAHs to BC. In previous free energy calculations [19], closely related molecules were slowly interconverted as a function of a

coupling parameter with procedures such as free energy perturbation, thermodynamic integration or slow growth. The procedures and applications of free energy calculations have been reviewed by Kollman [19]. The experimental value of the free energy of a structurally related compound functions as a reference state relative to which the free energy difference of a partition coefficient of a compound under study can be calculated. In this study, a hypothetical reference state was used that has equal free energies in both partitioning phases and will therefore cancel out in the calculated free energy difference. The reference state of the organic compound and partitioning phase that was chosen has no non-bonded van der Waals and electrostatic interactions and is assumed to be equal to the ideal gas phase. In this way, no experimental value of a strongly related compound or phase is required.

In this study, the Amber force field of Cornell et al. [20] was calibrated in order to properly simulate hydrated systems of polyaromatic condensed phases. Scaling factors for atomic charges of water and carbon-containing compounds were therefore derived by fitting results from Monte Carlo simulations obtained at different atomic charges to the experimental enthalpy of vaporisation of water and Bz, respectively. The BC or soot model structure ($C_{54}H_{18}$) used is a truncated symmetrical polyaromatic sheet of carbon mimicking the structure of soot and only takes surface adsorption of PAHs into account. This model structure is relatively small compared with, for example, the soot structure proposed by Akhter et al. [21], but was used to enable rapid force field calculations of relatively small molecular systems.

2. Theory

2.1 *Thermodynamic integration*

In this study, the statistical thermodynamical concept of the canonical ensemble is used for the calculation of sorption coefficients with molecular simulations [22]. This represents a hypothetical collection of systems simulating the many states a real system can possess in time, which all have a constant number of particles (N, number of molecules or moles), volume (V) and temperature (T). In a canonical ensemble, the difference in Helmholtz free energy, $\Delta F = F_1 - F_0$, between a studied system 1 and a reference state 0, follows from a thermodynamic integration procedure of the derivative of the mean potential energy to a coupling or variational parameter, λ (see [23]),

$$\Delta F = \int_{\lambda=0 \text{ to } 1} (\delta E/\delta\lambda)_\lambda \, d\lambda \tag{1}$$

where δE is the potential energy difference between system 1 and its reference state 0. In this approach, the coupling parameter changes the intermolecular and intramolecular non-bonded interactions from their original values to zero, which is hypothesised to represent the reference state. A linear dependence of E over the whole range of λ is not expected because molecular positions and orientations may gradually change during variation of the coupling parameter. It is therefore assumed that the dependence includes higher-order contributions:

$$E(\lambda) = B_0 + B_1 \cdot \lambda + B_2 \cdot \lambda^2 + B_3 \cdot \lambda^3 + B_4 \cdot \lambda^4 \tag{2}$$

The values of B_0 to B_4 can be determined by nonlinear regression of E as a function of λ. Integration of the Helmholtz free energy difference in Equation (2) gives

$$\Delta F = B_0 + \tfrac{1}{2} \cdot B_1 + \tfrac{1}{3} \cdot B_2 + \tfrac{1}{4} \cdot B_3 + \tfrac{1}{5} \cdot B_4 \tag{3}$$

The resulting free energy difference and the free energy of the reference state 0 can be used to calculate the unknown value of the system in its macroscopic state 1: $F_1 = \Delta F + F_0$. If a second system 2 is found with an identical reference state 0, the free energy difference between system 1 and 2 can be calculated without knowledge of the free energy of the reference state: $F_2 - F_1 = \Delta F_2 - \Delta F_1$.

2.2 *Sorption coefficients*

In order to calculate the mole fraction sorption coefficient ($K^x_{BA} = x_{eq,B}/x_{eq,A}$) for the partitioning of a sorbate C between water (A) and water containing a sorbent (B), the thermodynamic potential at infinite dilution (μ^∞_C) of a sorbate C dissolved in phase A (system 1: $N_A + 1_C$) or B (system 2: $N_B + 1_C$) is required. The sorption coefficient is explicitly termed a partitioning process here because the sorbate distributes over two distinct phases considering only surface adsorption takes place. In the case of the pure liquid phase A, the molar Gibbs free energy (G) can be assumed to be equal to the Helmholtz free energy:

$$G(N_A) = F(N_A) = \Delta F(N_A) + F(N_A)_{\lambda=0} \tag{4}$$

The liquid phase is simulated by inserting N_A molecules in the same V at the same T and $\Delta F(N_A)$ is subsequently calculated according to Equations (1)–(3). The molar free energy of A with only bonded intramolecular interactions is represented by $F(N_A)_{\lambda=0}$. The molar free energy of a sorbate C immersed in a large amount of water molecules ($N_A + 1_C$) will be

$$F(N_A + 1_C) = \Delta F(N_A + 1_C) + F(N_A + 1_C)_{\lambda=0} \tag{5}$$

and the thermodynamic potential at infinite dilution of C dissolved in A will become

$$\mu^\infty_{C,A} = F(N_A + 1_C) - F(N_A) = \Delta F(N_A + 1_C) + F(N_A + 1_C)_{\lambda=0} - [\Delta F(N_A) + F(N_A)_{\lambda=0}] \tag{6}$$

In the reference state at $\lambda = 0$, the solvent (N_A) and the sorbate dissolved in solvent ($N_A + 1_C$) have no intermolecular and intramolecular non-bonded interactions. The free energies of N_A and $N_A + 1_C$ will therefore only differ in the bonded (free) energy of the sorbate:

$$F(N_A + 1_C)_{\lambda=0} - F(N_A)_{\lambda=0} = F(C)_{A,\lambda=0} \tag{7}$$

The thermodynamic potential of C dissolved in water containing a sorbent ($N_B + 1_C$) is similar to Equation (6) assuming that the bonded intramolecular energies of C in A and B are equal, $F(C)_{A,\lambda=0} = F(C)_{B,\lambda=0}$. At $\lambda = 0$, the reference free energy is equal to the free energy of an ideal gas due to the absence of intermolecular interactions between the molecules. No corrections have to be applied, however, when the differences in reference free energies are calculated and the reference free energies are expressed in the molecular partition functions making use of Stirling's approximation (see [24]).

Therefore, the difference in the thermodynamic potentials of C dissolved in water containing a sorbent, $\mu^\infty_{C,B,}$ and dissolved in water only, $\mu^\infty_{C,A,}$ is related to the mole fraction sorption coefficient, K^x_{BA}. This difference is directly obtained from the thermodynamic integration of C in an aqueous environment with and without a sorbent

in which the sorbent should have a known molecular weight (with $R = 8.3144$ J/mol K and $T = 298.15$ K):

$$\mu^{\infty}_{C,B} - \mu^{\infty}_{C,A} = [\Delta F(N_B + 1_C) - \Delta F(N_B)] - [\Delta F(N_A + 1_C) - \Delta F(N_A)]$$
$$= \Delta F(C)_B - \Delta F(C)_A = -RT \operatorname{Ln} K^{x}_{BA} \quad (8)$$

3. Method

The procedure followed in the calculation of BC sorption coefficients that is described in more detail below consists of: (1) optimisation in the gas and hydrated phase of molecular structures for PAHs and/or BC; (2) scaling of atomic charges to obtain accurate charges in condensed systems for the calculation of free energies; (3) molecular simulation of hydrated structures with a gradual change of the structure to its reference state using a coupling parameter; and (4) calculation of the free energy difference by thermodynamic integration of simulated energies of transfer.

3.1 *Optimisation of gas and hydrated phase structures*

Molecular models of Bz, Phe, Fla, BaP and BC were geometrically optimised with a convergence limit (conv.) of 0.0004 kJ/mol *in vacuo* with the Amber force field from [20] with Hyperchem, version 7.51 [25]. The atomic charges for water, Phe, Fla, BaP and BC were calculated semi-empirically with PM3 in Hyperchem (conv. 0.0004 kJ/mol) and were subsequently changed with different scaling factors as described below. Geometrical optimisation (GO; Polak-Ribière optimisation; conv. 0.004 kJ/mol) was performed to obtain the starting structure for further optimisation.

The gas-phase optimised molecular structures were hydrated in periodic boxes of water ($x, y, z = 18.6451$ Å). For a system with constant volume, the total amount of water molecules ($N = 216$ for a periodic box containing only water) was decreased with the amount of water molecules, Z_Y and Z_X, corresponding to the molar volume of an added sorbate and/or sorbent ($N - Z_Y - Z_X = N - v_{sorbate}/v_{water} - v_{sorbent}/v_{water}$; Table 1). The molar volume of water, Bz and sorbates was calculated via $v = MW/d$ with density data taken from [26–28]. The calculated molar volumes were corrected to 25°C via $v(T, s) = v(25°C, s) \times [1 + 0.00025(T - 25)]$ where 0.00025 is a thermal expansion coefficient (in degrees^{-1}) of the solid compound (s) and T is the measurement temperature. The molar volume of the liquid compound (l) is subsequently calculated with the following equation,

Table 1. Experimental properties of water, benzene (Bz), phenanthrene (Phe), fluoranthene (Fla), benzo[*a*]pyrene (BaP) and black carbon (BC).

Property	*Water*	*Bz*	*Phe*	*Fla*	*BaP*	*BC*
Formula	H_2O	C_6H_6	$C_{14}H_{10}$	$C_{16}H_{10}$	$C_{20}H_{12}$	$C_{54}H_{18}$
MW (g/mol)	18.02	78.11	178.23	202.26	252.31	666.74
d^{temp} (g/cm^3)	0.9969^{25} (l)	0.8729^{25} (l)	1.174^{20} (s)	1.252^{2} (s)	1.351^{25} (s)	–
v (cm^3/mol)	18.07	89.49	162.16	172.43	196.25	436.21
$(N-Z_Y-Z_X)$*H_2O	216	–	207	206	205	192
Z_Y	–	–	9	10	11	–
Z_X	–	–	–	–	–	24

$v(25°C, l) = (0.98093 \pm 0.02697) \times v(25°C, s) + 13.051 \pm 2.654$, taken from [29]. The molar volume of BC was calculated from a QSAR equation, $v_m = 0.3024 \pm 0.007148 \times V(\text{Hyperchem}) - 11.95 \pm 3.383$ ($r^2 = 0.9819$; standard error of regression (SER) = 4.451; $N = 35$), where V(Hyperchem) is calculated with the QSAR option in Hyperchem for seven alkylated benzenes, six PAHs, four alkylated phenols, five ketones, four carboxylic acids, five alkylacetates, two alkylbenzoates, hexachloroethane and atrazine ranging in molar volume from $v = 74.03$ to 189.48 cm^3/mol.

All molecular mechanics calculations with GO, molecular dynamics (MD) and Monte Carlo simulations (MC) were performed with outer/inner switched summation cut-offs of 9/5 Å. A constant dielectric of $D = 1$ and scaling of close (1,4) intramolecular van der Waals and electrostatic non-bonded contributions by 0.5 was applied. The hydrated sorbate and/or sorbent was subjected to GO in two steps. First, the water molecules were selected only and GO was performed (conv. 0.04 kJ/mol). Second, GO was performed for the complete box including water and sorbate and/or sorbent (conv. 0.004 kJ/mol) and this structure was used for all subsequent optimisations.

The hydrated structures were optimised with threefold cyclic annealing (MD: heat/run/cool = 8/20/8 ps; $\Delta t = 0.0008$ ps, $\Delta T = 30$ K and a bath relaxation time, $\tau = 3.2$ ps). A long MD run (heat/run/cool = 8/600/0 ps; same settings as above) was subsequently performed for the cyclic annealing run that had the lowest energy after GO. The structure with the lowest GO energy was selected as the starting structure for the MC simulations. Optimisation of liquid Bz ($N = 27$; $x, y, z = [N.v/0.60221]^{1/3} = 21.1867$ Å; v from Table 1) and water ($N = 216$) with cyclic annealing and MD was only performed for the structure at $s = 1.0000$. The selected structure was subsequently used at other scaling factors after GO.

3.2 *Determination of atomic charge scaling factors*

The atomic charges of gaseous and liquid Bz ($N = 27$) or water ($N = 216$) were scaled to fit the experimental energy of vaporisation, ΔE_{vap}. At four different (squared) scaling factors for benzene ($s^2 = 0.3448 - 1.0000$) or water ($s^2 = 3.2860 - 5.4097$), MC energies were calculated for the gas and the liquid phase and the desired scaling factor was calculated. It was assumed that the energy of vaporisation has a linear relationship with s^2 as follows:

$$E_{gas} = B_{0,gas} + B_{1,gas} \cdot s^2 \tag{9}$$

$$E_{liq} = B_{0,liq} + B_{1,liq} \cdot s^2 \tag{10}$$

$$\Delta E_{vap} = E_{gas} - E_{liq} = \Delta B_0 + \Delta B_1 \cdot s^2 \tag{11}$$

The PM3 atomic charges of sorbates and sorbent or water were subsequently changed according to the scaling factor ($s = q/q_{PM3}$) derived from gas- and liquid-phase MC simulations of Bz or water, respectively.

3.3 *MC simulation*

The MC method as described elsewhere [30] is used to simulate the canonical ensemble. In this method, an exactly constant temperature is maintained and the kinetic (translational)

energy will therefore be constant. In the simulations, only the potential energy is allowed to vary. The potential energy E of a certain configuration [20,30] includes contributions of intramolecular stretching of bonds, bending of angles, torsion of (proper or improper) dihedral angles and intramolecular and intermolecular non-bonded interactions between atoms of the van der Waals and electrostatic type. The volume is held constant as the volume of a cubic periodic box in which the constant number of molecules is placed. Atomic coordinates (and bond lengths, bond angles, torsion angles and non-bonded distances) are varied randomly. Energies connected to these configurations are accepted only if they meet certain criteria. After averaging accepted energies, the macroscopic (mean) potential energy is found.

In the MC simulations, a coupling parameter was varied to decrease the electrostatic and non-bonded interactions to zero (reference state with $\lambda = 0$). The MC simulations were carried out at $\lambda = 1.0$, 0.8, 0.6, 0.4, 0.2 and 0.1 with the same starting structure. For each respective MC run, the atomic charges for the electrostatic interactions were decreased by multiplying with the squared root value of λ and the van der Waals minimum energy parameters for the non-bonded interactions (ε_{vdW} in parameter files of the force field) were decreased by multiplying with the corresponding λ values. After GO of the hydrated structures at each λ value, MC simulations were performed in 120,000 run steps (with maximum delta = 0.05 Å and at $T = 298.15$ K). During an MC run, the potential energy for the complete structure (E_{ABC}) was collected every two time steps (total of 60,000 data points). Snapshots were taken in intervals of 10 data steps in order to sample the total energy (E_{ABC}) and the individual energies of water molecules A ($E_{\underline{A}BC}$), sorbent B ($E_{A\underline{B}C}$) and sorbate C ($E_{AB\underline{C}}$) as well as combinations of these molecules ($E_{\underline{AB}C}$, $E_{A\underline{BC}}$ and $E_{\underline{A}B\underline{C}}$) with a script.

The sampled E_{ABC} data of the complete system (including water with sorbate and/or sorbent) were treated as follows. The E_{ABC} values were divided into 12 subgroups (sg) of 5000 data points. The averages of these subgroups were calculated and an exponential equation was fitted to the data:

$$E_{ABC} = B_0 + B_1 \cdot \exp(B_2 \cdot sg) \tag{12}$$

The equilibrium level was calculated as $B_0 \pm$ standard deviation (SD) and equilibrium was also determined visually. After equilibrium was achieved visually, the averages of two large groups of $E_{AB\underline{C}}$ data were calculated. The average and SD were subsequently calculated from the two averages.

The average E_{ABC} and $E_{AB\underline{C}}$ values determined for the individual MC runs and the GO energies of the starting system were plotted versus the coupling parameter and fitted using Equation (2) with the nonlinear regression option in Prism, version 3.02 [31]. With six E_{ABC} averages (from $\lambda = 0.1$ to 1.0), a maximum of four parameters were fitted for E_{ABC} and three parameters for $E_{AB\underline{C}}$. The parameters, B_0–B_4, were selected depending on the statistical significance of the individual parameters (SD) and the SER of the fit. The inaccuracy of ΔF was set equal to the SER.

3.4 *Sorption coefficients*

The contributions of all bonds in the system of water with sorbate and sorbent were dissected into intramolecular energies of the water (E_A), sorbent (E_B) and sorbate (E_C) molecules and the intermolecular energies between these molecules (E_{AA}, E_{AB}, E_{AC} and

E_{BC}), see Appendix 1. The energies E_{AXY}, E_{AXC}, E_{ABY} and E_{ABC} are the energies of the systems of bulk liquid water, water containing sorbate, sorbent, and sorbate in combination with sorbent, respectively. When a sorbate C is introduced in the canonical ensembles of phases A and B, the number of molecules N changes with $-Z+1$, and a correction has to be applied to account for the loss of water molecules from the system. The following assumptions are made for the calculation of the sorption coefficient, K_{BC}. (i) The infinitely diluted solution can be approximated by a relatively small box with a limited number of molecules. (ii) Kinetic energy effects can be neglected or will cancel in the comparison of systems when the systems are at a constant temperature of 298.15 K (constant T). (iii) The molar volumes of the solution are assumed to be ideal, showing no contraction or expansion with respect to the unmixed phases. Therefore, the cavity created has a molar volume equal to the molar volume of sorbent B and/or sorbate C ($v_B = Z_X \cdot v_A$; $v_C = Z_Y \cdot v_A$) (constant V). (iv) The potential energy of Z_X, Z_Y or $Z_X + Z_Y$ solvent molecules considered as molecules in the pure solvent system are added to the potential energies of the systems of dissolved sorbate and/or sorbent (constant N). (v) All intramolecular structures and energies will be similar in each system. (vi) The intermolecular interactions between molecules of the same type are considered to be equal in each system.

Under assumption (iv), the energy contributions to the thermodynamic potentials of the sorbate in pure solvent, $e_{C,A}$, and in solvent containing a sorbent, $e_{C,B}$ are corrected with $Z_Y/N \cdot E_{AXY}$ and $(Z_X + Z_Y)/N \cdot E_{AXY}$ as follows:

$$e_{C,A} = E_{AXC} + Z_Y/N \cdot E_{AXY} - E_{AXY} \tag{13}$$

$$e_{C,B} = E_{ABC} + (Z_X + Z_Y)/N \cdot E_{AXY} - [E_{ABY} + Z_X/N \cdot E_{AXY}] \tag{14}$$

When assumptions (v) and (vi) are taken into account, the thermodynamic potentials of sorbates in water and in water containing a sorbent are equal at equilibrium leading to the following expression:

$$e_{C,B} - e_{C,A} = E_{AB\underline{C}} - E_{AX\underline{C}} - E_{BY} + E_{XY} \tag{15}$$

Equation (15) contains a contribution of the difference in the interaction between the sorbent with the Z_Y water molecules replaced by the sorbate (E_{BY}) and the interaction between Z_Y water molecules with the Z_X water molecules replaced by the sorbent (E_{XY}). The thermodynamic integration of these energy terms over the coupling parameter, $\lambda = 0$–1, leads to the free energy difference from which the mole fraction sorption coefficient can be calculated using Equation (8).

4. Results and discussion

4.1 *Scaling of atomic charges*

At different scaling factors, charges of Bz and water were changed as described in Section 3 and MC simulations were performed after GO (see Appendix 2). Results for the difference between gas- and liquid-phase energies (in kJ/mol) of Bz are given in Equation (16) and the desired scaling factor was calculated from the experimental ΔE_{vap} value. In this way, a scaling factor of $s_{Bz} = 0.9502 \pm 0.0099$ was calculated for Bz from $\Delta E_{vap,exp} = 31.35 \pm 0.07$ kJ/mol ($\Delta H_{vap,exp} = 33.83 \pm 0.07$ kJ/mol from Chickos and Acree [32]; $\Delta E_{vap,exp} = \Delta H_{vap,exp} - RT$). This scaling factor was subsequently used to downscale

the PM3 atomic charges (by $q = s_{Bz} \cdot q_{PM3}$) of PAHs and BC for further calculations. A $\Delta E_{vap,Bz}$ value of $E_{MC,gas} - E_{MC,liq} = 31.14$ kJ/mol was subsequently calculated (see the row in italics in Appendix 2) corresponding to the experimental value.

$$\Delta E_{vap,\,Bz} = (19.1698 \pm 0.1439) + (13.4967 \pm 0.1996) \cdot s^2 \quad \text{SER} = 0.126 \qquad (16)$$

For water, a scaling factor of $s_{H_2O} = 1.8363 \pm 0.019$ was calculated with a similar procedure using Equation (17) and $\Delta E_{vap,exp} = 41.51 \pm 0.07$ kJ/mol ($\Delta H_{vap,exp} = 43.99 \pm 0.07$ kJ/mol from Chickos and Acree [32]). This scaling factor was used to upscale the atomic charges of water ($q_O = -0.6584$ and $q_H = 0.3292$). This results in a $\Delta E_{vap,H_2O}$ value of 41.22 kJ/mol (see the row in italics in Appendix 2) and is only 0.29 kJ/mol lower than the experimental value.

$$\Delta E_{vap,\,H_2O} = (-18.4322 \pm 0.4711) + (17.7778 \pm 0.1146) \cdot s^2 \quad \text{SER} = 0.188 \qquad (17)$$

The resulting mean atomic charges for the aromatic carbon atoms in Phe ($q_C = -0.071$ e), Fla ($q_C = -0.073$ e) and BaP ($q_C = -0.060$ e) and the exterior aromatic carbon atoms in BC ($q_C = -0.076$ e) are less negative than the aromatic carbon atoms present in Bz ($q_C = -q_H = -0.097$ e).

4.2 *Free energy contribution*

Averages of the MC potential energies for the hydrated structures have been calculated with Equation (12) and values at $\lambda = 1.0$ are shown in Table 2. The averages of selected PAHs have been calculated by taking the average of two large groups where equilibrium was achieved visually. The standard deviations at $\lambda = 1.0$ of selected Phe, Fla and BaP are much lower than the energy of the complete structure (Table 2 and Appendix 3 for all λ values). The MC potential energies of selected Phe and Fla as a function of λ are shown in Figure 1 (BaP is not shown for clarity) and they show a maximum at low λ values. The calculated free energy Fla obtained from fitting Equation (2) results into high inaccuracies of SER = 16.44 to 29.46 kJ/mol in ΔF for the hydrated structure (data not shown), whereas ΔF of the selected sorbate has much lower inaccuracies of SER = 4.35 to 4.39 kJ/mol (Appendix 4).

Table 2. Monte Carlo potential energies of selected molecules (in kJ/mol; energy ± standard deviation).

System	E_{ABC}	$E_{\underline{A}BC}$	$E_{AB\underline{C}}$	E_B	E_C
Water	−8101.48 ± 12.97	–	–	–	–
BC	−6723.60 ± 15.52	156.57 ± 8.58	–	496.06 ± 21.13	–
Phe	−7774.08 ± 13.76	–	12.20 ± 2.20	–	134.59 ± 13.98
BCPhe	−6248.59 ± 8.32	117.16 ± 13.91	−49.40 ± 1.56	497.92 ± 19.95	129.00 ± 22.88
Fla	−7523.00 ± 9.54	–	86.32 ± 2.72	–	223.26 ± 21.21
BCFla	−6239.81 ± 9.87	109.70 ± 9.20	25.56 ± 0.46	492.29 ± 12.93	213.09 ± 13.47
BaP	−7645.67 ± 7.45	–	28.27 ± 11.91	–	183.54 ± 21.89
BCBaP	−6193.78 ± 12.74	113.24 ± 1.26	−45.50 ± 3.88	509.00 ± 20.63	191.49 ± 20.43

Notes: $E_B = E_{ABC} - E_{\underline{A}B\underline{C}}$; $E_C = E_{ABC} - E_{\underline{AB}C}$.

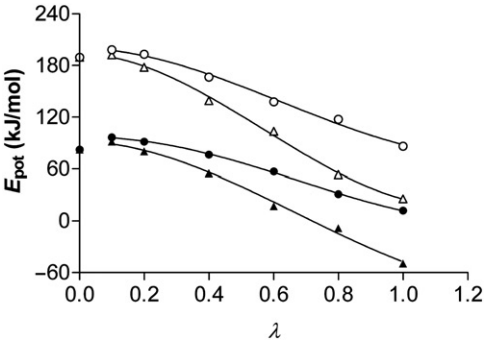

Figure 1. Equilibrium Monte Carlo potential energies for phenanthrene and fluoranthene as a function of the coupling parameter, λ (● $E_{Phe,pot}$ water; ▲ E_{BCPhe} water with BC; ○ E_{Fla} water; △ E_{BCFla} water with BC; plotted standard deviations are smaller than symbols).

Table 3. Free energy differences of selected molecules (in kJ/mol; ± standard error of regression) and BC sorption coefficients calculated in this study and from literature (in L/kg C; ± standard error).

Compound	*Phe*	*Fla*	*BaP*
$\Delta F_{AB\underline{C}}$	33.92 ± 5.08	117.65 ± 4.35	49.43 ± 3.03
$\Delta F_{AX\underline{C}}$	62.69 ± 1.09	151.96 ± 4.39	88.68 ± 1.60
ΔF_{BY}	−6.64 ± 0.29	−7.36 ± 0.33	−8.11 ± 0.36
ΔF_{XY}	−16.25 ± 0.27	−18.07 ± 0.29	−19.86 ± 0.33
log K_{BC}			
This study	5.17 ± 0.54	6.33 ± 0.64	7.38 ± 0.36
Diesel soot	5.68 [5], 6.12 [17]	6.93 [17]	8.97 [17]
Sediments	6.1, 5.6 [34], 5.65 [35]	6.4, 6.5 [34], 6.28 [35]	7.1, < 7.4 [34], 7.22 [35]
QSAR	6.02 [7], 5.73 [37]	6.48 [7], 6.48 [37]	7.11 [7], 7.51 [37]

4.3 *Sorption coefficients*

The free energy differences between (selected) PAHs in water containing BC and in water were calculated by combining Equations (8) and (15) and are shown in Table 3 and Appendix 4. The calculated free energy differences ($\Delta F_C = \Delta G$) were subsequently converted into mole-fraction-based sorption coefficients, $K^x = \exp(-\Delta G/RT)$. The sorption coefficients (log K_{BC}; expressed in L/kg C) were calculated from the K^x values via

$$\log K_{BC} = \log\left(\frac{v_w}{MW_C N_C} K^x\right) \tag{18}$$

where v_w is the molar volume of water (Table 1), MW_C is the molecular weight of carbon (12.011 g/mol) and N_C is the number of carbon atoms ($N_C = 54$) in BC. The standard error (SE) in log K_{BC} reported in Table 3 was calculated from the (error propagated) SER of individual free energy contributions via SE = SER/ln (10). The resulting log K_{BC} values are a factor of 3 to 39 times lower than literature values for diesel soot reported by Bucheli and Gustafsson [5] for added Phe determined by equilibration through headspace ($c_w = 1$ μg/L; 134 days) and by Jonker and Koelmans [17] for native PAHs determined with a

polyoxomethylene partitioning method ($c_w = 0.03$ – 200 ng/L (see [33]); 28 days). The diesel soot was obtained in these studies as a standard reference material (SRM1650) from the National Institute of Standards and Technology (NIST, Gaithersburg, MD). The calculated log K_{BC} values of Fla and BaP are however in agreement with values reported by Lohmann et al. [34] for native PAHs in two harbour sediments determined with a polyethylene partitioning method ($c_w = 0.01$ – 1.10 μg/L; 182 and 14 days). In addition, Hawthorne et al. [35] reported mean log K_{BC} values of native PAHs by determining sediment and porewater concentrations (median $c_w = < 0.01 - 0.48$ μg/L) of 47 to 103 sediments impacted by manufactured gas plant activities and aluminium smelters that also correspond closely to calculated log K_{BC} values of Fla and BaP. The log K_{BC} value calculated for Phe in this study is within a factor of three to nine of literature values reported for natural sediments. Furthermore, BC sorption coefficients of PAHs for aquatic sediments gave a linear relationship to the octanol to water partition coefficient (log K_{ow}) of PAHs: $\log K_{BC} = 0.6997 \times \log K_{ow} + 2.8219$ (see [7]) that resulted into log K_{BC} values for Fla and BaP similar to values calculated in this study (Table 3). The log K_{ow} values used in this equation were taken from [36]. Finally, the calculated log K_{BC} values for Fla and BaP are in close agreement with log K_{BC} values estimated from a linear relationship to both log K_{ow} and the specific surface area (SSA) of soot derived for PAHs, chlorobenzenes, non and mono-*ortho* polychlorinated biphenyls (PCBs), $\log K_{BC} = 1.14 \times \log K_{ow} + 1.72 - \log 998/\text{SSA}$ (see [37]). The SSA used in this equation was taken from [6] and represents a median literature value ($\text{SSA} = 63\ m^2/g$; $n = 12$). This relationship was derived from estimation of sorption affinities (b) and maximum adsorption capacities (Q_{max}) in the initial linear part of a Langmuir isotherm (where $K_{BC} = b \times Q_{max}$) [37] assuming that monolayer adsorption is dominating at low concentrations. It is assumed in this estimation method that interactions between PAHs and soot are equal to interactions between PAHs in the solid phase [37].

4.4 *Interactions between PAHs and black carbon*

The energies of separate molecules (water, sorbate and sorbent) and combinations of these molecules were selected in Hyperchem (see Appendix 5) and the energy values for E_{ABC}, $E_{A\underline{B}C}$ and $E_{AB\underline{C}}$ are shown in Table 2. The contributions of the intramolecular and intermolecular energies to the total energy were subsequently calculated from these selected energies (Appendices 1 and 6). The intramolecular energy of the sorbate does not change in the aqueous phase with and without BC (E_C in Table 2). The same applies for the sorbent molecule (E_B in Table 2). This would imply that sorption of PAHs to BC only involves intermolecular interactions. In molecular simulations performed by Kubicki [16], the main mechanism of interaction between PAHs and soot was attributed to van der Waals forces between the Π electrons within the aromatic rings of both PAHs and soot.

The total potential energies of (selected) Fla and BC were additionally dissected into contributions of non-bonded and electrostatic energy. The total potential energy decreases from 86.32 ± 2.72 to 25.56 ± 0.46 kJ/mol for Fla and from 156.57 ± 8.58 to 109.70 ± 9.20 kJ/mol for BC. The energetic gain is due to a decrease in non-bonded van der Waals energy by -69.45 ± 2.26 and -57.61 ± 6.28 kJ/mol for Fla and BC, respectively. The electrostatic energy increases by 9.62 ± 3.64 and 13.51 ± 10.33 kJ/mol for Fla and BC, respectively, and represents the energy loss due to fewer interactions between sorbate or sorbent and nearest water molecules. The remaining energy difference of + 0.92 for Fla

and −3.35 for BC is due to small changes in intramolecular stretching of bonds, bending of angles and torsion of dihedral angles.

The distance between PAHs and BC during the MC simulations (calculated at $\lambda = 1.0$ with gOpenMol [38], version 3.00) averaged around 3.85 Å (Phe), 3.66 Å (Fla) and 3.68 Å (BaP) and is in agreement with previous modelling calculations by Kubicki [15,16] where a spacing distance of 3.5 Å between PAHs and soot models was observed. The calculated distances between PAHs and BC are remarkably similar to the interlayer spacing distance (4.1 Å) between polyaromatic planes of diesel soot from the NIST determined with high-resolution transmission electron microscopy [39]. The larger distance between Phe and BC could explain its lower sorption coefficient calculated in this study, because the strength of dispersive interactions between hydrophobic sorbates and BC depends on the separation distance between sorbate and sorbent [40].

5. Final remarks

In the natural environment, elevated total organic matter sorption coefficients are observed at low sorbate concentrations in the nanograms per litre level and they are decreased at higher sorbate concentrations in the micrograms per litre level due to saturation of BC sorption sites [5,41]. The thermodynamic potentials calculated in this study are assumed to be valid at infinite dilution and the calculated log K_{BC} values therefore should approximate the literature values that are measured or estimated at low sorbate concentrations in the absence of competition between sorbates. The literature values from [17] measured at concentrations at and above nanograms per litre levels for diesel soot are however higher than the log K_{BC} values calculated in this study indicating underestimation of PAH sorption located both on surfaces and in micropores of diesel soot. This suggests that the used BC structure only functions as a suitable probe model structure that mimics the mainly non-bonded nature of surface adsorption of petrogenic PAHs (sorbed after deposition of BC) to soot. Larger models of soot (e.g. the soot model from Akhter et al. [21]) would be required to obtain mechanistic information on the location of adsorption of pyrogenic PAHs (coproduced with soot) in micropores.

The proposed free energy procedure applied in this study using MC simulations has the advantage that long equilibration times necessary for measurement of log K_{BC} values in the laboratory are circumvented. In addition, this method provides structural information on the interactions involved in the sorption process which is not given by other existing estimation methods. In the case of surface adsorption, the method can be extended to other PAHs for which experimental values are missing. With an appropriate charge model, the method can further be applied to compounds with varying polarity and planarity for which experimental log K_{BC} values are available [42]. In addition, the method can be tested to simulate interactions of polar or apolar sorbates with organic macromolecules such as humic or fulvic acids.

Acknowledgement

The present study was supported by the European Commission, project ABACUS (Evaluation of Availability to Biota for Organic Compounds Ubiquitous in Soils and Sediments - EVK1-2001-00101).

References

[1] H.A.J. Govers, H.B. Krop, J.R. Parsons, T. Tambach, and J.D. Kubicki, *Dissolved organic carbon–contaminant interaction descriptors found by 3D force field calculations*, SAR QSAR Environ. Res. 13 (2002), pp. 271–280.

[2] H.A.J. Govers, A. Van Roon, and J.R. Parsons, *Calculation of the interaction between dissolved organic carbon and organic micropollutants by three dimensional force field methods*, Environ. Toxicol. Chem. 22 (2003), pp. 753–759.

[3] H.A.J. Govers, P. De Voogt, O. Kwast, and E.A.J. Bleeker, *Membrane–contaminant interaction found by 3D force field calculations*, SAR QSAR Environ. Res. 13 (2002), pp. 135–143.

[4] A. Van Roon, J.R. Parsons, and H.A.J. Govers, *Cytochrome P450cam–monoterpene interactions. Prediction of product profiles for monoterpene hydroxylation using a calibrated 3D force field*, SAR QSAR Environ. Res. 16 (2005), pp. 369–384.

[5] T.D. Bucheli and Ö. Gustafsson, *Quantification of the soot–water distribution coefficient of PAHs provides mechanistic basis for enhanced sorption observations*, Environ. Sci. Technol. 34 (2000), pp. 5144–5151.

[6] G. Cornelissen, Ö. Gustafsson, T.D. Bucheli, M.T.O. Jonker, A.A. Koelmans, and P.C.M. Van Noort, *Extensive sorption of organic compounds to black carbon, coal, and kerogen in sediments and soils: Mechanisms and consequences for distribution, bioaccumulation, and biodegradation*, Environ. Sci. Technol. 39 (2005), pp. 6881–6895.

[7] A.A. Koelmans, M.T.O. Jonker, G. Cornelissen, T.D. Bucheli, P.C.M. Van Noort, and Ö. Gustafsson, *Black carbon: the reverse of its dark side*, Chemosphere 63 (2006), pp. 365–377.

[8] J.D. Kubicki and S.E. Apitz, *Models of natural organic matter and interactions with organic contaminants*, Org. Geochem. 30 (1999), pp. 911–927.

[9] H.-R. Schulten, *Interactions of dissolved organic matter with xenobiotic compounds: molecular modeling in water*, Environ. Toxicol. Chem. 18 (1999), pp. 1643–1655.

[10] M.S. Diallo, J.-L. Faulon, W.A. Goddard III, and J.H. Johnson Jr, *Binding of hydrophobic organic compounds to dissolved humic substances: a predictive approach based on computer assisted structure elucidation, atomistic simulations and Flory–Huggins solution theory*, in *Humic Substances: Structures, Models and Functions*, E.A. Ghabbour and G. Davies, eds., The Royal Society of Chemistry, Cambridge, 2001, pp. 221–237.

[11] H.-R. Schulten, M. Thomsen, and L. Carlsen, *Humic complexes of diethyl phthalate: molecular modelling of the sorption process*, Chemosphere 45 (2001), pp. 357–369.

[12] J.D. Kubicki and C.C. Trout, *Molecular modeling of fulvic and humic acids: charging effects and interactions with Al^{3+}, benzene, and pyridine*, in *Geochemical and hydrological reactivity of heavy metals in soils*, W.L. Kingery and H.M. Selim, eds., CRC Press, Boca Raton, FL, 2003, pp. 113–143.

[13] C. Niederer and K.U. Goss, *Quantum chemical modeling of humic acid/air equilibrium partitioning of organic vapors*, Environ. Sci. Technol. 41 (2007), pp. 3646–3652.

[14] C.C. Trout and J.D. Kubicki, *Molecular modeling of Al^{3+} and benzene interactions with Suwannee fulvic acid*, Geochim. Cosmochim. Acta 71 (2007), pp. 3859–3871.

[15] J.D. Kubicki, *Molecular mechanics and quantum mechanical modeling of hexane soot and interactions with pyrene*, Geochem. Trans. 7 (2000), pp. 41–46.

[16] J.D. Kubicki, *Molecular simulations of benzene and PAH interactions with soot*, Environ. Sci. Technol. 40 (2006), pp. 2298–2303.

[17] M.T.O. Jonker and A.A. Koelmans, *Sorption of polycyclic aromatic hydrocarbons and polychlorinated biphenyls to soot and soot-like materials in the aqueous environment: Mechanistic considerations*, Environ. Sci. Technol. 36 (2002), pp. 3725–3734.

[18] D. Frenkel and B. Smit, *Understanding Molecular Simulation: From Algorithms To Applications*, 2nd ed., Academic Press, San Diego, CA, 2002.

[19] P. Kollman, *Free-energy calculations—applications to chemical and biochemical phenomena*, Chem. Rev. 93 (1993), pp. 2395–2417.
[20] W.D. Cornell, P. Cieplak, C.I. Bayly, I.R. Gould, K.M. Merz, D.M. Ferguson, D.C. Spellmeyer, T. Fox, J.W. Caldwell, and P.A. Kollman, *A second generation force field for the simulation of proteins, nucleic acids, and organic molecules*, J. Am. Chem. Soc. 117 (1995), pp. 5179–5197.
[21] M.S. Akhter, A.R. Chughtai, and D.M. Smith, *The structure of hexane soot I: Spectroscopic studies*, Appl. Spectrosc. 39 (1985), pp. 143–153.
[22] N.A. Gocken and R.G. Reddy, *Thermodynamics*, Plenum Press, New York, 1996.
[23] T.P. Lybrand, *Computer simulation of biomolecular systems using molecular dynamics and free energy perturbation methods*, in *Reviews in Computational Chemistry*, K.B. Lipkowitz and D.B. Boyd, eds., VCH, New York, 1990, pp. 295–321.
[24] C.J. Cramer, *Essentials of Computational Chemistry*, *Theories and Models*, Wiley, New York, 2002.
[25] *Hyperchem 7.51*, Hypercube Inc., Gainsville, FL, 2004.
[26] D. MacKay, W.Y. Shiu, and K.C. Ma, *Illustrated Handbook of Physical–Chemical Properties and Environmental Fate for Organic Chemicals*, Lewis Publishers, Boca Raton, FL, 1992.
[27] International Programme on Chemical Safety, *Selected Non-heterocyclic Polycyclic Aromatic Hydrocarbons*, *Environmental Health Criteria 202*, World Health Organization, Geneva, 1998.
[28] D.R. Lide, *Handbook of Chemistry and Physics*, CRC Press, Boca Raton, FL, 2000.
[29] H.A.J. Govers and P. De Voogt, *Gas chromatographic derivation of the solubility parameters of polychlorinated biphenyls with the inclusion of cis–trans and optical isomerism and orientational disorder*, SAR QSAR Environ. Res. 3 (1995), pp. 315–324.
[30] J.-P. Doucette and J. Weber, *Computer-aided Molecular Design*, Academic Press, London, 1997.
[31] *Prism 3.02*, Graphpad Software, San Diego, CA, 2000.
[32] J.S. Chickos and W.E. Acree, *Enthalpies of vaporization of organic and organometallic compounds, 1880–2002*, J. Phys. Chem. Ref. Data 32 (2003), pp. 519–878.
[33] P.C.M. Van Noort, M.T.O. Jonker, and A.A. Koelmans, *Modeling maximum adsorption capacities of soot and soot-like materials for PAHs and PCBs*, Environ. Sci. Technol. 38 (2004), pp. 3305–3309.
[34] R. Lohmann, J.K. MacFarlane, and P.M. Gschwend, *Importance of black carbon to sorption of native PAHs, PCBs and PCDDs in Boston and New York harbor sediments*, Environ. Sci. Technol. 39 (2005), pp. 141–148.
[35] S.B. Hawthorne, C.B. Grabanski, and D.J. Miller, *Measured partitioning coefficients for parent and alkyl polycyclic aromatic hydrocarbons in 114 historically contaminated sediments: part 2. Testing the $K_{oc}K_{BC}$ two carbon-type model*, Environ. Toxicol. Chem. 26 (2007), pp. 2505–2516.
[36] P.G.J. De Maagd, D.T.E.M. Ten Hulscher, H. Van den Heuvel, A. Opperhuizen, and D.T.H.M. Sijm, *Physicochemical properties of polycyclic aromatic hydrocarbons: aqueous solubilities, n-octanol/water partition coefficients, and Henry's law constants*, Environ. Toxicol. Chem. 17 (1998), pp. 251–257.
[37] P.C.M. Van Noort, *A thermodynamic-based estimation model for adsorption of organic compounds by carbonaceous materials in environmental sorbents*, Environ. Toxicol. Chem. 22 (2003), pp. 1179–1188.
[38] D.L. Bergman, L. Laaksonen, and A. Laaksonen, *Visualization of solvation structures in liquid mixtures*, J. Mol. Graphics Modell. 15 (1997), pp. 301–306.
[39] Ö. Gustafsson, T.D. Bucheli, Z. Kukulska, M. Andersson, C. Largeau, J.N. Rouzaud, C.M. Reddy, and T.I. Eglinton, *Evaluation of a protocol for the quantification of black carbon in sediments*, Global Biogeochem. Cycles 15 (2001), pp. 881–890.
[40] R.P. Schwarzenbach, P.M. Gschwend, and D.M. Imboden, *Environmental Organic Chemistry*, 2nd ed., Wiley, New York, 2003.

[41] G. Cornelissen, Z. Kukulska, S. Kalaitzidis, K. Christanis, and Ö. Gustafsson, *Relations between environmental black carbon sorption and geochemical sorbent characteristics*, Environ. Sci. Technol. 38 (2004), pp. 3632–3640.

[42] G. Cornelissen, J. Haftka, J. Parsons, and Ö. Gustafsson, *Sorption to black carbon of organic compounds with varying polarity and planarity*, Environ. Sci. Technol. 39 (2005), pp. 3688–3694.

Appendix 1

Here we list the contributions of energies in the molecular systems of pure solvent (A) and solutions of sorbate (C) and/or sorbent (B) in solvent.

Notation

N = number of water molecules
Z_X = number of water molecules equal to molar volume of sorbent B
Z_Y = number of water molecules equal to molar volume of sorbate C
E_A, E_B and E_C = intramolecular energy of A, B and C

Selected molecules are underlined.

System 0	System 1	System 2	System 3
A A A A A A	A A A A A A A	A A A A A A A	A A A A A A A
A Y X X X A	A X X X A	A Y A	A A A
A Y X X X A	A C X X X A	A Y B A	A C B A
A Y X X X A	A X X X A	A Y A	A A A
A A A A A A	A A A A A A A	A A A A A A A	A A A A A A A
A A A A A A	A A A A A A A	A A A A A A A	A A A A A A A

System 0: Pure solvent A at N, V, T;

$$E_{AXY} = (N - Z_X - Z_Y)\cdot E_A + E_{AA} + Z_X E_A + Z_Y E_A + E_{AX} + E_{AY} + E_{XX} + E_{XY} + E_{YY}$$

$$E_{\underline{A}XY} = (N - Z_X - Z_Y)\cdot E_A + E_{AA} + E_{AX} + E_{AY}$$

$$E_{A\underline{X}Y} = + Z_X \cdot E_A + E_{XA} + E_{XX} + E_{XY}$$

$$E_{AX\underline{Y}} = + Z_Y \cdot E_A + E_{YA} + E_{YX} + E_{YY}$$

$$E_{\underline{AX}Y} = (N - Z_X - Z_Y)\cdot E_A + E_{AA} + Z_X \cdot E_A + E_{AX} + E_{AY} + E_{XX} + E_{XY}$$

$$E_{A\underline{XY}} = + Z_X \cdot E_A + Z_Y \cdot E_A + E_{AX} + E_{AY} + E_{XX} + E_{XY} + E_{YY}$$

$$E_{\underline{AXY}} = (N - Z_X - Z_Y)\cdot E_A + E_{AA} + Z_Y \cdot E_A + E_{AX} + E_{AY} + E_{XY} + E_{YY}$$

$$E_{AA} = {}^1/_2 \Sigma_{i=1-N-Zx-Zy}\ \Sigma_{i'\neq i=1-N-Zx-Zy}\ A_i A_{i'}$$

$$E_{AX} = \Sigma_{i=1-N-Zx-Zy}\ \Sigma_{j=1-Zx} A_i X_j = E_{XA} = \Sigma_{i=1-Zx}\Sigma_{j=1-N-Zx-Zy} X_i A_j$$

$$E_{AY} = \Sigma_{i=1-N-Zx-Zy}\Sigma_{j=1-Zy} A_i Y_j = E_{YA} = \Sigma_{i=1-Zy}\Sigma_{j=1-N-Zx-Zy} Y_i A_j$$

$$E_{XX} = {}^1/_2 \Sigma_{i=1-Zx}\Sigma_{i'\neq i=1-Zx} X_i X_{i'}$$

$$E_{XY} = \Sigma_{i=1-Zx}\Sigma_{j=1-Zy} X_i Y_j = E_{YX} = \Sigma_{i=1-Zy}\Sigma_{j=1-Zx} Y_i X_j$$

$$E_{YY} = {}^1/_2 \Sigma_{i=1-Zy}\Sigma_{i'\neq i=1-Zy} Y_i Y_{i'}$$

$$AA0 = {}^1/_2 \Sigma_{i=1-N}\Sigma_{i'\neq i=1-N} A_i A_{i'} = E_{AA} + E_{AX} + E_{AY} + E_{XX} + E_{XY} + E_{YY}$$

$$E_{\mathrm{AX\underline{Y}}} = (N - Z_{\mathrm{Y}})/N \cdot E_{\mathrm{AXY}}$$
$$E_{\mathrm{A\underline{XY}}} = (N - Z_{\mathrm{X}} - Z_{\mathrm{Y}})/N \cdot E_{\mathrm{AXY}}$$
$$\mathrm{AA0} = E_{\mathrm{AXY}} - N \cdot E_{\mathrm{A}}$$
$$E_{\mathrm{XY}} = [(Z_{\mathrm{X}} \cdot Z_{\mathrm{Y}})/(N \cdot N)] \cdot \mathrm{AA0}$$

System 1: Solution of C in solvent A at $N{-}Z_{\mathrm{Y}}+1$, V, T;

$$\begin{aligned}
E_{\mathrm{AXC}} &= (N - Z_{\mathrm{X}} - Z_{\mathrm{Y}}) \cdot E_{\mathrm{A}} + E_{\mathrm{AA}} + Z_{\mathrm{X}} E_{\mathrm{A}} + E_{\mathrm{C}} + E_{\mathrm{AX}} + E_{\mathrm{AC}} + E_{\mathrm{XX}} + E_{\mathrm{XC}} \\
E_{\mathrm{\underline{A}XC}} &= (N - Z_{\mathrm{X}} - Z_{\mathrm{Y}}) \cdot E_{\mathrm{A}} + E_{\mathrm{AA}} + E_{\mathrm{AX}} + E_{\mathrm{AC}} \\
E_{\mathrm{A\underline{X}C}} &= + Z_{\mathrm{X}} \cdot E_{\mathrm{A}} + E_{\mathrm{XA}} + E_{\mathrm{XX}} + E_{\mathrm{XC}} \\
E_{\mathrm{AX\underline{C}}} &= + E_{\mathrm{C}} + E_{\mathrm{CA}} + E_{\mathrm{CX}} \\
E_{\mathrm{\underline{AC}X}} &= (N - Z_{\mathrm{X}} - Z_{\mathrm{Y}}) \cdot E_{\mathrm{A}} + E_{\mathrm{AA}} + Z_{\mathrm{X}} \cdot E_{\mathrm{A}} + E_{\mathrm{AX}} + E_{\mathrm{AC}} + E_{\mathrm{XX}} + E_{\mathrm{XC}} \\
E_{\mathrm{A\underline{CX}}} &= + Z_{\mathrm{X}} \cdot E_{\mathrm{A}} + E_{\mathrm{C}} + E_{\mathrm{AX}} + E_{\mathrm{AC}} + E_{\mathrm{XX}} + E_{\mathrm{XC}} \\
E_{\mathrm{\underline{A}X\underline{C}}} &= (N - Z_{\mathrm{X}} - Z_{\mathrm{Y}}) \cdot E_{\mathrm{A}} + E_{\mathrm{AA}} + E_{\mathrm{C}} + E_{\mathrm{AX}} + E_{\mathrm{AC}} + E_{\mathrm{XC}}
\end{aligned}$$

$$E_{\mathrm{AA}} = {}^1\!/_2 \Sigma_{\mathrm{i=1-N-Zx-Zy}} \Sigma_{\mathrm{i' \neq i=1-N-Zx-Zy}} \mathrm{A_i A_{i'}}$$
$$E_{\mathrm{AX}} = \Sigma_{\mathrm{i=1-N-Zx-Zy}} \Sigma_{\mathrm{j=1-Zy}} \mathrm{A_i X_j} = E_{\mathrm{XA}} = \Sigma_{\mathrm{i=1-Zy}} \Sigma_{\mathrm{j=1-N-Zx-Zy}} \mathrm{X_i A_j}$$
$$E_{\mathrm{AC}} = \Sigma_{\mathrm{i=1-N-Zx-Zy}} \mathrm{A_i C} = E_{\mathrm{CA}} = \Sigma_{\mathrm{j=1-N-Zx-Zy}} \mathrm{C A_j}$$
$$E_{\mathrm{XX}} = {}^1\!/_2 \Sigma_{\mathrm{i=1-Zx}} \Sigma_{\mathrm{i \neq i=1-Zx}} \mathrm{X_i X_{i'}}$$
$$E_{\mathrm{XC}} = \Sigma_{\mathrm{i=1-Zx}} \mathrm{X_i C} = E_{\mathrm{CX}} = \Sigma_{\mathrm{j=1-Zx}} \mathrm{C X_j}$$

$$E_{\mathrm{C}} = E_{\mathrm{AXC}} - E_{\mathrm{\underline{A}X\underline{C}}}$$

System 2: Solution of B in solvent A at $N{-}Z_{\mathrm{X}}+1$, V, T;

$$\begin{aligned}
E_{\mathrm{ABY}} &= (N - Z_{\mathrm{X}} - Z_{\mathrm{Y}}) \cdot E_{\mathrm{A}} + E_{\mathrm{AA}} + E_{\mathrm{B}} + Z_{\mathrm{Y}} E_{A} + E_{\mathrm{AB}} + E_{\mathrm{AY}} + E_{\mathrm{BY}} + E_{\mathrm{YY}} \\
E_{\mathrm{\underline{A}BY}} &= (N - Z_{\mathrm{X}} - Z_{\mathrm{Y}}) \cdot E_{\mathrm{A}} + E_{\mathrm{AA}} + E_{\mathrm{AB}} + E_{\mathrm{AY}} \\
E_{\mathrm{A\underline{B}Y}} &= + E_{\mathrm{B}} + E_{\mathrm{AB}} + E_{\mathrm{BY}} \\
E_{\mathrm{AB\underline{Y}}} &= + Z_{\mathrm{Y}} \cdot E_{\mathrm{A}} + E_{\mathrm{AY}} + E_{\mathrm{BY}} + E_{\mathrm{YY}} \\
E_{\mathrm{\underline{AB}Y}} &= (N - Z_{\mathrm{X}} - Z_{\mathrm{Y}}) \cdot E_{\mathrm{A}} + E_{\mathrm{AA}} + E_{\mathrm{B}} + E_{\mathrm{AB}} + E_{\mathrm{AY}} + E_{\mathrm{BY}} \\
E_{\mathrm{A\underline{BY}}} &= + E_{\mathrm{B}} + Z_{\mathrm{Y}} \cdot E_{\mathrm{A}} + E_{\mathrm{AB}} + E_{\mathrm{AY}} + E_{\mathrm{BY}} + E_{\mathrm{YY}} \\
E_{\mathrm{\underline{A}B\underline{Y}}} &= (N - Z_{\mathrm{X}} - Z_{\mathrm{Y}}) \cdot E_{\mathrm{A}} + E_{\mathrm{AA}} + Z_{\mathrm{Y}} \cdot E_{\mathrm{A}} + E_{\mathrm{AB}} + E_{\mathrm{AY}} + E_{\mathrm{BY}} + E_{\mathrm{YY}}
\end{aligned}$$

$$E_{\mathrm{AA}} = {}^1\!/_2 \Sigma_{\mathrm{i=1-N-Zx-Zy}} \Sigma_{\mathrm{i' \neq i=1-N-Zx-Zy}} \mathrm{A_i A_{i'}}$$
$$E_{\mathrm{AY}} = \Sigma_{\mathrm{i=1-N-Zx-Zy}} \Sigma_{\mathrm{j=1-Zy}} \mathrm{A_i Y_j} = E_{\mathrm{YA}} = \Sigma_{\mathrm{i=1-Zy}} \Sigma_{\mathrm{j=1-N-Zx-Zy}} \mathrm{Y_i} A_{\mathrm{j}}$$
$$E_{\mathrm{AB}} = \Sigma_{\mathrm{i=1-N-Zx-Zy}} \mathrm{A_i B} = E_{\mathrm{BA}} = \Sigma_{\mathrm{j=1-N-Zx-Zy}} \mathrm{B A_j}$$
$$E_{\mathrm{YY}} = {}^1\!/_2 \Sigma_{\mathrm{i=1-}Z_y} \Sigma_{\mathrm{i' \neq i=1-Zy}} \mathrm{Y_i Y_{i'}}$$
$$E_{\mathrm{YB}} = \Sigma_{\mathrm{i=1-Zy}} \mathrm{Y_i B} = \mathrm{E_{BY}} = \Sigma_{\mathrm{j=1-Zy}} \mathrm{B Y_j}$$

$$E_{\mathrm{B}} = E_{\mathrm{ABY}} - E_{\mathrm{\underline{A}B\underline{Y}}}$$
$$E_{\mathrm{BY}} = Z_{\mathrm{Y}}/(N - Z_{\mathrm{X}}) \cdot (E_{\mathrm{A\underline{B}Y}} - E_{\mathrm{ABY}} + E_{\mathrm{\underline{A}B\underline{Y}}})$$

System 3: Solution of C in solvent A + B at $N-Z_X-Z_Y+2$, V, T;

$$
\begin{array}{lllllll}
E_{ABC} = & (N-Z_X-Z_Y)\cdot E_A & +E_{AA} & +E_B & +E_C & +E_{AB} & +E_{AC} & +E_{BC} \\
E_{\underline{A}BC} = & (N-Z_X-Z_Y)\cdot E_A & +E_{AA} & & & +E_{AB} & +E_{AC} & \\
E_{A\underline{B}C} = & & & +E_B & & +E_{AB} & & +E_{BC} \\
E_{AB\underline{C}} = & & & & +E_C & & +E_{AC} & +E_{BC} \\
E_{\underline{AB}C} = & (N-Z_X-Z_Y)\cdot E_A & +E_{AA} & +E_B & & +E_{AB} & +E_{AC} & +E_{BC} \\
E_{\underline{A}B\underline{C}} = & & & +E_B & +E_C & +E_{AB} & +E_{AC} & +E_{BC} \\
E_{\underline{AB}\underline{C}} = & (N-Z_X-Z_Y)\cdot E_A & +E_{AA} & & +E_C & +E_{AB} & +E_{AC} & +E_{BC}
\end{array}
$$

$$
\begin{aligned}
E_{AA} &= {}^1\!/_2 \Sigma_{i=1-N-Zx-Zy} \Sigma_{i' \neq i=1-N-Zx-Zy} A_i A_{i'} \\
E_{AB} &= \Sigma_{i=1-N-Zx-Zy} A_i B = E_{BA} = \Sigma_{j=1-N-Zx-Zy} B A_j \\
E_{AC} &= \Sigma_{i=1-N-Zx-Zy} A_i C = E_{CA} = \Sigma_{j=1-N-Zx-Zy} C A_j
\end{aligned}
$$

$$
\begin{aligned}
(-Z_X-Z_Y)\cdot E_A + E_{AA} &= E_{ABC} - E_{\underline{A}B\underline{C}} \\
E_B &= E_{ABC} - E_{\underline{A}B\underline{C}} \\
E_C &= E_{ABC} - E_{\underline{AB}C} \\
E_{AB} &= E_{ABC} - E_{AB\underline{C}} - [(N-Z_X-Z_Y)\cdot E_A + E_{AA}] - E_B \\
&= (E_{ABC} - E_{AB\underline{C}}) - (E_{ABC} - E_{A\underline{B}\underline{C}}) - (E_{ABC} - E_{\underline{A}B\underline{C}}) \\
&= -E_{ABC} - E_{A\underline{B}\underline{C}} + E_{\underline{A}B\underline{C}} + E_{\underline{A}B\underline{C}} \\
E_{AC} &= E_{ABC} - E_{A\underline{B}C} - [(N-Z_X-Z_Y)\cdot E_A + E_{AA}] - E_C \\
&= (E_{ABC} - E_{A\underline{B}C}) - (E_{ABC} - E_{A\underline{B}C}) - (E_{ABC} - E_{\underline{A}BC}) \\
&= -E_{ABC} - E_{A\underline{B}C} + E_{\underline{A}BC} + E_{\underline{A}BC} \\
E_{BC} &= E_{ABC} - E_{\underline{A}BC} - E_B - E_C \\
&= (E_{ABC} - E_{\underline{A}BC}) - (E_{ABC} - E_{\underline{A}B\underline{C}}) - (E_{ABC} - E_{\underline{A}BC}) \\
&= -E_{ABC} - E_{\underline{A}BC} + E_{\underline{A}B\underline{C}} + E_{\underline{A}BC}
\end{aligned}
$$

Appendix 2

The following table lists the MC potential energies (in kJ/mol) of benzene and water at different values of s^2. A theoretical value of 3.7179 kJ/mol ($3.\!{}^1\!/_2 .RT$) was used for the MC potential energy for gaseous water ($E_{MC,gas}$) as six out of the possible nine degrees of freedom are used for the rotation and translation of the molecule in the gas phase.

s^2		$E_{MC,gas}$	$E_{MC,liq}$
Benzene	q_H		
1.0000	0.1021	57.053 ± 0.017	24.292 ± 0.063
0.8955	0.0966	56.384 ± 0.017	25.246 ± 0.008
0.3999	0.0646	53.300 ± 0.008	28.652 ± 0.013
0.3448	0.0600	52.936 ± 0.021	29.167 ± 0.033
Water	q_O		
5.4097	−0.834	3.7179	-73.981 ± 0.000
3.8766	−0.706	3.7179	-46.852 ± 0.059
3.5374	−0.6744	3.7179	-40.861 ± 0.075
3.3719	−0.6584	3.7179	-37.505 ± 0.059
3.2860	−0.650	3.7179	-36.070 ± 0.042

Appendix 3

The following table lists the equilibrium MC potential energies (in kJ/mol; standard deviation given) of hydrated Phe, Fla and BaP, hydrated BC with Phe, Fla and BaP and energetic contributions from hydrated black carbon (E_{BY}) and water (E_{XY}).

λ	H_2OPhe $E_{AX\underline{C}}$	H_2OBCPhe $E_{AB\underline{C}}$	H_2OBC (Phe) E_{BY}	H_2O (BCPhe) E_{XY}
0.0[a]	82.26 ± 0.09	82.26 ± 0.09	-	-
0.1	96.62 ± 1.16	91.66 ± 0.91	0.47 ± 0.14	−0.24 ± 0.05
0.2	91.59 ± 0.36	80.47 ± 1.73	−0.95 ± 0.71	−2.83 ± 0.08
0.4	76.71 ± 1.05	55.09 ± 0.61	−4.37 ± 0.99	−10.00 ± 0.02
0.6	57.19 ± 1.01	17.23 ± 1.51	−8.11 ± 2.34	−19.19 ± 0.15
0.8	31.20 ± 0.46	−8.36 ± 3.13	−12.55 ± 2.49	−30.07 ± 0.02
1.0	12.20 ± 2.20	−49.40 ± 1.56	−15.91 ± 1.07	−42.01 ± 0.06
	H_2OFla $E_{AX\underline{C}}$	H_2OBCFla $E_{AB\underline{C}}$	H_2OBC (Fla) E_{BY}	H_2O (BCFla) E_{XY}
0.0[a]	189.49 ± 0.00	189.49 ± 0.00	–	–
0.1	198.32 ± 2.09	192.25 ± 2.13	0.50 ± 0.17	−0.25 ± 0.04
0.2	193.18 ± 0.59	177.90 ± 1.09	−1.05 ± 0.79	−3.14 ± 0.08
0.4	166.65 ± 0.71	139.12 ± 1.46	−4.85 ± 1.09	−11.13 ± 0.04
0.6	137.95 ± 3.26	103.60 ± 1.42	−9.00 ± 2.59	−21.34 ± 0.17
0.8	117.53 ± 0.25	53.72 ± 1.00	−13.93 ± 2.76	−33.39 ± 0.00
1.0	86.32 ± 2.72	25.56 ± 0.46	−17.70 ± 1.17	−46.69 ± 0.08
	H_2OBaP $E_{AX\underline{C}}$	H_2OBCBaP $E_{AB\underline{C}}$	H_2OBC (BaP) E_{BY}	H_2O (BCBaP) E_{XY}
0.0[a]	112.00 ± 0.03	112.00 ± 0.03	–	–
0.1	129.73 ± 1.39	120.25 ± 0.43	0.57 ± 0.17	−0.30 ± 0.06
0.2	123.57 ± 0.17	104.79 ± 0.88	−1.16 ± 0.86	−3.46 ± 0.10
0.4	104.71 ± 1.01	74.22 ± 2.18	−5.35 ± 1.21	−12.22 ± 0.03
0.6	82.21 ± 1.74	35.89 ± 2.36	−9.91 ± 2.85	−23.46 ± 0.18
0.8	51.05 ± 1.92	−10.77 ± 3.34	−15.33 ± 3.05	−36.75 ± 0.02
1.0	28.27 ± 11.91	−45.50 ± 3.88	−19.45 ± 1.31	−51.34 ± 0.08

[a]Calculated from the individual MC potential energies of water molecules, sorbate and sorbent at $\lambda = 0$. Gas phase molecules with zero charges were inserted into periodic boxes of water dimensions and MC simulation of 5,000,000 run steps was carried out. The data were collected every 100 time steps (total of 50,000 data points) and all ε_{vdW} values were set to 0.00001.

Appendix 4

The following table list the parameters of free energy fitting (standard deviations given) of MC results for hydrated Phe, Fla, BaP, BC with Phe, Fla and BaP and calculated free energy contributions ($\Delta F \pm$ standard error of regression).

Parameter	H_2OPhe $E_{AX\underline{C}}$	H_2OBCPhe $E_{AB\underline{C}}$	H_2OBC (Phe) E_{BY}	H_2O (BCPhe) E_{XY}
B_0	97.34 ± 0.78	91.44 ± 3.89	0.52 ± 0.22	2.48 ± 0.34
B_1				-23.08 ± 1.53
B_2	-131.86 ± 4.64	-274.12 ± 36.83	-36.76 ± 2.12	-21.56 ± 1.37
B_3		135.40 ± 36.35	20.36 ± 2.09	
B_4	46.54 ± 4.57			
ΔF	62.69 ± 1.09	33.92 ± 5.08	-6.64 ± 0.29	-16.25 ± 0.27
	H_2OFla $E_{AX\underline{C}}$	H_2OBCFla $E_{AB\underline{C}}$	H_2OBC (Fla) E_{BY}	H_2O (BCFla) E_{XY}
B_0	199.74 ± 3.39	193.43 ± 3.31	0.59 ± 0.25	2.76 ± 0.38
B_1				-25.65 ± 1.72
B_2	-238.86 ± 31.97	-405.18 ± 31.46	-40.84 ± 2.34	-23.97 ± 1.51
B_3	127.32 ± 31.55	237.15 ± 31.09	22.64 ± 2.34	
B_4				
ΔF	151.96 ± 4.39	117.65 ± 4.35	-7.36 ± 0.33	-18.07 ± 0.29
	H_2OBaP $E_{AX\underline{C}}$	H_2OBCBaP $E_{AB\underline{C}}$	H_2OBC (BaP) E_{BY}	H_2O (BCBaP) E_{XY}
B_0	130.32 ± 1.15	120.49 ± 2.32	0.64 ± 0.27	3.03 ± 0.41
B_1				-28.21 ± 1.86
B_2	-159.02 ± 6.82	-354.47 ± 21.96	-44.93 ± 2.59	-26.36 ± 1.68
B_3		188.42 ± 21.68	24.88 ± 2.56	
B_4	56.83 ± 6.72			
ΔF	88.68 ± 1.60	49.43 ± 3.03	-8.11 ± 0.36	-19.86 ± 0.33

Appendix 5

The following table lists the MC potential energies (in kJ/mol) of selected water, solute and/or sorbent molecules.

Selected energies	H_2O E_{AXY}	H_2OPhe E_{AXC}	H_2OFla E_{AXC}	H_2OBaP E_{AXC}
E_{AXC}	-8101.48 ± 12.97	-7774.08 ± 13.76	-7523.00 ± 9.54	-7645.67 ± 7.45
$E_{AX\underline{C}}$		12.20 ± 2.20	86.32 ± 2.72	28.27 ± 11.91
$E_{\underline{A}X\underline{C}}$		-7908.68 ± 2.44	-7746.26 ± 18.95	-7829.21 ± 20.58
	H_2OBC E_{ABY}	H_2OBCPhe E_{ABC}	H_2OBCFla E_{ABC}	H_2OBCBaP E_{ABC}
E_{ABC}	-6723.60 ± 15.52	-6248.59 ± 8.32	-6239.81 ± 9.87	-6193.78 ± 12.74
$E_{\underline{A}BC}$		-6816.56 ± 18.41	-6885.32 ± 9.04	-6807.34 ± 15.95
$E_{A\underline{B}C}$	156.57 ± 8.58	117.16 ± 13.91	109.70 ± 9.20	113.24 ± 1.26
$E_{AB\underline{C}}$		-49.40 ± 1.56	25.56 ± 0.46	-45.50 ± 3.88
$E_{\underline{A}\underline{B}C}$		-6377.60 ± 21.32	-6452.90 ± 9.20	-6385.27 ± 15.97
$E_{A\underline{B}\underline{C}}$		127.55 ± 12.42	197.69 ± 9.41	149.82 ± 3.19
$E_{\underline{A}B\underline{C}}$	-7219.66 ± 14.35	-6746.52 ± 18.13	-6732.10 ± 8.37	-6702.79 ± 16.22

Appendix 6

In the following table the energy contributions (in kJ/mol) of selected water, solute and/or sorbent molecules are listed. In the contributions, N, Z_X and Z_Y denote amount of water molecules in the presence of only water (A), sorbent (B) or sorbate (C), respectively;

$$\mathrm{AA0} = E_{\mathrm{total}} - N \cdot E_{\mathrm{A}};$$

$$(N - Z_{\mathrm{X}} - Z_{\mathrm{Y}}) \cdot E_{\mathrm{A}} + E_{\mathrm{AA}} = E_{\mathrm{total}} - E_{\mathrm{B}} - E_{\mathrm{C}} - E_{\mathrm{AB}} - E_{\mathrm{AC}} - E_{\mathrm{BC}};$$

$$E_{\mathrm{B}} = E_{\mathrm{ABY}} - E_{\underline{\mathrm{A}}\underline{\mathrm{BY}}}; E_{B} = E_{\mathrm{ABC}} - E_{\underline{\mathrm{A}}\underline{\mathrm{BC}}};$$

$$E_{\mathrm{C}} = E_{\mathrm{AXC}} - E_{\underline{\mathrm{AX}}\underline{\mathrm{C}}}; E_{\mathrm{C}} = E_{\mathrm{ABC}} - E_{\underline{\mathrm{ABC}}};$$

$$E_{\mathrm{AB}} = -E_{\mathrm{ABC}} - E_{\mathrm{AB}\underline{\mathrm{C}}} + E_{\underline{\mathrm{A}}\mathrm{BC}} + E_{\underline{\mathrm{AB}}\mathrm{C}};$$

$$E_{\mathrm{AC}} = -E_{\mathrm{ABC}} - E_{\mathrm{A}\underline{\mathrm{BC}}} + E_{\underline{\mathrm{A}}\mathrm{BC}} + E_{\underline{\mathrm{AB}}\mathrm{C}};$$

$$E_{\mathrm{BC}} = -E_{\mathrm{ABC}} - E_{\underline{\mathrm{A}}\mathrm{BC}} + E_{\underline{\mathrm{A}}\mathrm{B}\underline{\mathrm{C}}} + E_{\underline{\mathrm{AB}}\mathrm{C}};$$

$$E_{\mathrm{water}}(N = 1) = E_{\mathrm{AXY}}/N; E_{\underline{\mathrm{AX}}\underline{\mathrm{C}}}/(N - Z_{\mathrm{Y}}); E_{\underline{\mathrm{A}}\underline{\mathrm{BY}}}/(N - Z_{\mathrm{X}}); E_{\underline{\mathrm{A}}\underline{\mathrm{BC}}}/(N - Z_{\mathrm{X}} - Z_{\mathrm{Y}}).$$

Contributions	H_2O E_{AXY}	H_2OPhe E_{AXC}	H_2OFla E_{AXC}	H_2OBaP E_{AXC}
E_C		134.59 ± 13.98	223.26 ± 21.21	183.54 ± 21.89
E_{water} $(N=1)$	-37.49 ± 0.04	-38.21 ± 0.01	-37.61 ± 0.08	-38.19 ± 0.10
AA0	-9072.50 ± 13.26			
	H_2OBC E_{ABY}	H_2OBCPhe E_{ABC}	H_2OBCFla E_{ABC}	H_2OBCBaP E_{ABC}
$(N-Z_X-Z_Y).E_A + E_{AA}$		-6376.98 ± 60.07	-6440.01 ± 37.32	-6338.75 ± 53.11
E_B	496.06 ± 21.13	497.92 ± 19.95	492.29 ± 12.93	509.00 ± 20.63
E_C		129.00 ± 22.88	213.09 ± 13.47	191.49 ± 20.43
E_{AB}		-320.97 ± 23.55	-320.16 ± 16.02	-313.68 ± 21.23
E_{AC}		-118.61 ± 29.52	-125.14 ± 18.87	-154.91 ± 20.72
E_{BC}		-58.96 ± 34.51	-59.87 ± 18.28	-86.93 ± 30.58
E_{water} $(N=1)$	-37.61 ± 0.08	-37.25 ± 0.10	-37.82 ± 0.04	-37.61 ± 0.09